[PROC. OF JSCE Structural Eng./Earthquake Eng. Vol. 2, No. 2 October 1985]

PREDICTION OF NONSTATIONARY EARTHQUAKE MOTIONS ON ROCK SURFACE

By Masata SUGITO and Hiroyuki KAMEDA***

Nonstationary earthquake motion prediction models are proposed on the basis of rock surface-ground motion dataset. Ground motions on rock surface with the shear velocity of 600 ~700 m/sec are dealt with. The ninety-one components of acceleration time histories on rock surface level are arranged, which consist of (i) rock surface-ground motions estimated from the accelerograms recorded on alluvial and diluvial sites, (ii) rock surface-ground motions modified from bed rock ground motions, and (iii) ground motions recorded on rock surface. On the basis of this dataset, two earthquake motion prediction models are developed, one (EMP-IB Model), a prediction model for given magnitude and epicentral distance, and the other (EMP-IIB Model), an advanced model which deals with the effect of successive faulting and relative site locations on ground motion characteristics.

1. INTRODUCTION

Prediction of earthquake motions at specific sites for given earthquake scale and source-to-site distance is a significant subject in earthquake engineering. Theoretical calculation procedure by dynamic faulting model[6] can simulate ground motions which correspond to ground motions in relatively low frequency range, such as $f<0.1$ Hz. However, it is still very hard to simulate theoretical ground motions in high frequency range such as $f>0.1$ Hz, because it needs detailed information about local soil structures as well as local fault dynamic process.

In the fields of engineering researches where the verification of the model refered to the real data is indispensable, many statistical models for ground motions have been proposed by using various kinds of strong motion datasets. They mainly dealt with peak acceleration[17], prak velocity[17], and acceleration response spectra[10),18),19], as a function of earthquake magnitude M, and epicentral distance Δ (or hypocentral distance R). Earthquake motion prediction models have also been proposed[8),11),29], in which grornd motion characteristics such as spectral intensity, duration, nonstationarity, etc. were scaled for magnitude and distance.

In use of these prediction models the following problems may be pointed out. First, a large statistical uncertainty remains in the models because the strong motion data, which consist of relatively high frequency components as $f>0.1$ Hz, are strongly affected by the characteristics of local soil conditions as well as fault contact irregularity. Second, these statistical models are mainly based on weak ground motion data recorded on soil surface overlying bedrock. Therefore, these models cannot be applied for the case of large ground motions, where the nonlinear characteristics of overlying soils strongly affect ground motion

* Meber of JSCE, M. Eng., Research Associate, Kyoto University.
** Member of JSCE, Dr. Eng., Associate Professor, Kyoto University.

intensities. As for the former problem, the estimation formulas for 4 types of soil conditions prescribed in the design code for bridges[9] have been proposed to evaluate the local soil effects. A soil parameter S_n determined from SPT blow-count profiles has been used in the estimation formulas to account for the effect of local site conditions on ground motion intensities[12]. However, nonlinear characteristics of soil deposits during great earthquakes, which correspond to the latter problem, can not be solved by using only the weak ground motion data recorded on soil-overlying ground.

In this view of the problem, the nonstationary earthquake motion prediction models have been proposed by using rock surface-ground motion dataset, most of which have been modified from soil surface ground motion records. Significance of the prediction model for rock surface is as follows. (1) The model can be applied for earthquake resistant design of significant structures including nuclear opwer plants which are built on rock ground, and (2) the model is also useful for earthquake motion prediction for layered grounds by using the given rock surface motions as the input of the bed rock, where the amplification effect and nonlinear characteristics of overlying soils can be considered.

2. STRONG MOTION DATASET ON ROCK SURFACE[24]

(1) Definition of Rock Surface

For engineering purposes rock surface with the shear velocity v_s=700 m/s has been dealt with by Hisada, Ohsaki, Watabe, and Ohta[7], and the design spectra for significant structures including nuclear power plants have been proposed. In the present study nearly the same level of rock formations as Ref. 7) has been dealt with. Fig. 1 shows a schematic illustration for free rock surface and other related site conditions. Point A represents an imaginal case where overlying deposites are removed, and Point A' is an actual case for free rock surface. For other cases ground motions can be used after some appropriate modifications such as response analysis of soil layers (E), of irregular ground (C), and of soil structure interactions (B, D).

(2) Strong Motion Dataset on Free Rock Surface

Strong motion data used in this paper consist of 91 components of accelerograms which have been recorded at 17 stations during 26 Japanese earthquakes. These accelerograms have been corrected for baseline and instrument characteristics[1]. Table 1 shows the items of the data which are classified into 3 groups. The data from the group A and B have been modified into rock surface ground motions using soil profile data[30] for strong motion observation stations. Procedure of modifications for each group of the data are as follows.

a) Elimination of surface wave motions and response analysis of soil-overlying ground (Group A)

The data for group A consists of 77 components of accelerograms recorded on 12 alluvial and diluvial sites. Evolutionary spectra[13] for these data have been examined as for participation of surface wave motions. In 16 motions of the data in group A, surface wave motions were removed by a simple technique to separate body and surface waves[27]. The parameters t_d and f_d used for the separation are listed in Table 2. Earthquake motions on bed rock level were calculated using the soil profile data for the stations. Multi-reflection technique and equivalent linear model have been used for the ground response analysis. It is similar to the SHAKE program developed by Schnabel, Lysmer, and Seed[25]. However, the effect of ground motion duration on the effective shear strain γ_e has been incorporated in the following formula.

$$\gamma_e=0.6(T_d/T_m)^{0.1}\gamma_{\max} \quad \cdots\cdots (1)$$

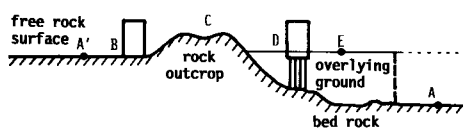

Fig. 1 Illustration of Bed Rock and Free Rock Surface.

Table 1 Classification of Strong Motion Dataset.

contents	No. of record components	No. of sites
A; records on the surface of grounds overlying bed rocks	77	12
B; records at underground bed rocks	8	3
C; records on rock surface	6	2

Table 2 Rock Surface Strong Motion Dtaset.

No.	Rec.No.	M	Δ	Comp.	Amax	Amax (free rock)	f_d^*	t_d^*	Category**
1	S-213	7.5	110.0	NS	213.4	120.4	-	-	A
2				EW	282.2	174.5	-	-	
3	S-234	7.9	293.0	NS	216.1	175.6	-	-	A
4				EW	245.1	138.0	-	-	
5	S-235	7.9	247.0	NS	252.0	253.2	0.5	25.5	A
6				EW	191.9	165.1	0.5	25.5	
7	S-236	7.9	189.0	NS	167.0	85.3	-	-	A
8				EW	160.3	88.4	-	-	
9	S-241	7.4	196.0	NS	117.4	70.0	-	-	A
10				EW	90.7	61.3	-	-	
11	S-252	7.9	235.0	NS	264.1	181.4	0.5	28.0	A
12				EW	203.3	201.7	0.5	28.0	
13	S-264	7.4	193.0	NS	80.8	57.1	0.7	20.0	A
14				EW	98.6	60.1	0.7	20.0	
15	S-271	7.4	213.0	EW	147.1	67.9	-	-	A
16				NS	121.3	57.2	-	-	
17	S-340	6.1	49.7	NS	87.1	43.1	-	-	A
18				EW	130.9	47.1	-	-	
19	S-453	6.5	52.0	NS	96.5	65.6	-	-	A
20				EW	124.8	90.5	-	-	
21	S-537	5.7	12.0	NS	170.6	82.5	-	-	A
22				EW	152.7	82.3	-	-	
23	S-544	6.7	53.2	NS	145.8	102.0	1.2	7.5	A
24				EW	143.5	147.9	1.2	7.5	
25	605-GR-26	4.8	21.0	NS	-	122.9	-	-	C
26				EW	-	137.5	-	-	
27	308-GR-2	7.5	103.0	LG	194.0	191.2	-	-	A
28				TR	209.3	248.1	-	-	
29	308-GR-8	5.3	18.3	TR	190.6	159.7	-	-	A
30				LG	256.0	264.3	-	-	
31	308-GR-4	6.6	18.7	TR	543.4	491.1	-	-	A
32				LG	600.6	475.6	-	-	
33	S-1204	7.4	166.7	EW	160.6	94.3	-	-	A
34				NS	223.0	123.8	-	-	
35	S-1201	7.4	100.0	NS	316.7	185.8	-	-	A
36				EW	281.7	239.5	-	-	
37	S-1210	7.4	103.0	N41E	-	180.1	-	-	C
38				E41S	-	210.4	-	-	
39	S-1202	7.4	273.0	NS	77.6	47.3	0.62	17.0	A
40				EW	68.7	38.2	0.62	17.0	
41	S-1058	7.0	80.9	E33S	54.3	32.7	0.3	50.0	A
42				S33W	62.7	25.9	0.3	50.0	
43	302-GR-34	6.7	85.8	LG	97.0	111.0	-	-	B
44				TR	170.7	186.6	-	-	
45	302-GR-35	7.4	82.7	LG	315.5	338.0	-	-	B
46				TR	394.4	410.5	-	-	
47	S-1463	5.3	70.0	EW	31.2	23.5	-	-	A
48				NS	48.8	38.0	-	-	
49	S-1470	5.5	57.0	EW	57.4	33.5	-	-	A
50				NS	60.7	23.6	-	-	
51	S-1474	7.1	137.0	NS	159.9	103.4	-	-	A
52				EW	180.5	121.3	-	-	
53	S-1494	6.1	63.0	S15W	-	28.4	-	-	C
54				W15N	-	53.4	-	-	
55	S-1497	6.1	110.0	EW	46.1	23.8	-	-	A
56				NS	53.6	28.4	-	-	
57	S-1505	7.0	124.0	EW	111.8	48.4	-	-	A
58				NS	93.5	49.5	-	-	
59	S-1509	7.0	207.0	E03N	30.4	12.7	-	-	A
60				S03E	29.8	12.1	-	-	
61	S-1514	7.0	251.0	EW	30.5	24.7	-	-	A
62				NS	23.8	18.4	-	-	
63	S-1518	5.7	64.0	W33N	23.3	14.5	-	-	A
64				N33E	42.3	20.0	-	-	
65	S-1519	5.7	64.0	E33S	48.9	20.4	-	-	A
66				S33W	82.4	33.7	-	-	
67	S-1521	5.3	49.0	EW	43.1	27.6	-	-	A
68				NS	34.3	23.0	-	-	
69	S-1526	5.3	79.0	EW	54.5	46.1	-	-	A
70				NS	21.3	16.8	-	-	
71	S-1528	4.8	25.0	EW	62.8	30.2	-	-	A
72				NS	90.9	54.3	-	-	
73	S-1532	5.1	48.0	EW	28.0	13.9	-	-	A
74				NS	34.6	13.3	-	-	
75	S-1571	7.7	270.0	EW	28.6	17.6	-	-	A
76				NS	37.6	18.8	-	-	
77	S-1573	7.7	156.0	EW	149.5	192.3	0.38	31.0	A
78				NS	117.3	96.7	0.33	56.0	
79	S-1592	7.1	160.0	EW	72.7	40.8	0.23	43.0	A
80				NS	59.0	37.3	0.45	55.6	
81	S-1599	7.1	201.0	EW	68.0	36.3	-	-	A
82	M-521	7.1	64.0	NS	143.5	70.9	-	-	A
83				EW	275.6	119.2	-	-	
84	M-522	5.8	59.0	NS	26.9	9.1	-	-	A
85				EW	33.1	13.8	-	-	
86	M-540	5.2	59.0	NS	61.8	25.9	-	-	A
87				EW	64.7	30.5	-	-	
88	M-546	6.1	75.0	N07W	15.0	16.6	-	-	B
89				E07N	13.9	14.9	-	-	
90	M-574	5.3	77.0	NS	11.5	12.6	-	-	B
91				EW	8.4	11.9	-	-	

*separation parameters for elimination of surface wave (Ref.27)
**corresponds to the contents in Table 1

where γ_{max}=maximum shear strain, T_d= ground motion duration defined by Vanmarke and Lai[33] ($T_d=7.7\,P_t/A_p^2$, P_t= acceleration total power and A_p= peak acceleration), and T_m= mean value of T_d for the data (herein T_d=6.9 s). The effective strain γ_e takes 0.5~0.7 γ_{max} depending on the duration T_d of the strong motion data. For the relation between shear modulus and strain level, the experimantal formulas proposed by Hardin and Drnevich[5] have been applied. After several times of iterative calculation (within 5 % error for the maximum shear strain), input motions on rock level were obtained. Then, corresponding rock surface ground motions are given by multiplying the input motions by two.

b) Response analysis of soil layers for the data recorded at underground bed rock (Group B)

8 components of the data in Group B have been obtained by underground accelerographs at 3 sites during 4 earthquakes. The input amplitudes of bed rock ground motions have been calculated by using the same response analysis procedure as

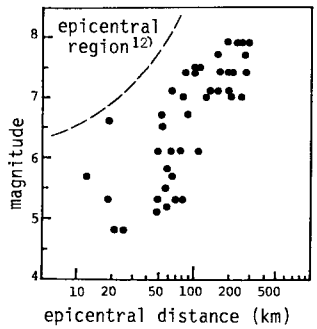

Fig. 2 Scattergram of Magnitude and Epicentral Distance.

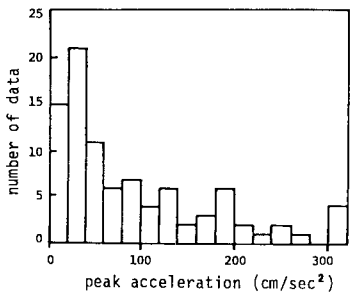

Fig. 3 Histogram of Peak Acceleration for Rock Surface Strong Motion Dataset.

described above. Then corresponding free rock surface motions have been obtained.

c) Records on rock surface (Group C)

6 components of the data in Group C have been obtained at 2 rock sites during 3 earthquakes. They have been included in the dataset without any modification.

The strong motion dataset on rock surface, arranged as described above, are listed in Table 2. The scattergram of magnitude and epicentral distance are shown in Fig. 2. The broken line in Fig. 2 shows the boundary of epicentral regions[12] where the ground motion intensities can be regarded not to depend on the epicentral distance. Fig. 3 shows the histogram of peak acceleration for rock surface strong motion dataset.

3. NONSTATIONARY EARTHQUAKE MOTION PREDICTION MODEL ON FREE ROCK SURFACE FOR GIVEN MAGNITUDE AND DISTANCE (EMP-I B Model)

(1) Simulation of Ground Motions by Evolutionary Process and Regression Analysis of Model Parameters on Magnitude M and Epicentral Distance Δ

Based on the 91 components of rock surface-strong motion dataset explained in Chapter 2, the earthquake motion prediction model for given magnitude and epicentral distance has been proposed. The procedure to complete the model is same as that developed by Kameda, Sugito, and Asamura[11] in which a prediction model for soil site motions has been proposed.

Earthquake acceleration with nonstationary frequency content can be represented by

$$x(t)=\sum_{k=1}^{m}\sqrt{2G_x(t,\omega_k)\Delta\omega}\cdot\cos(\omega_k\cdot t+\varphi_k) \quad \cdots\cdots (2)$$

in which $G_x(t, \omega_k)$ =evolutionary spectrum for time t and angular frequency ω_k, φ_k= independent random phaze angles distributed over $0\sim 2\pi$, and m=number of superposed harmonic components. The upper and lower boundary frequencies f_u, f_l are fixed as f_u= 10.03 Hz, f_l=0.13 Hz, and also m and Δf $(=\Delta\omega/2\pi)$ are fixed as m=166 and Δf= 0.06 Hz. The following time-varying function is adopted for the model of $G_x(t, \omega_k)$.

$$\sqrt{G_x(t,\omega)}=\sqrt{G_x(t,2\pi f)}=\begin{cases}0 & ;0\leqq t<t_s(f)\\ \alpha_m(f)\left\{\dfrac{t-t_s(f)}{t_p(f)}\right\}\exp\left\{1-\dfrac{t-t_s(f)}{t_p(f)}\right\} & ;t\geq t_s(f)\end{cases} \quad \cdots\cdots (3)$$

in which $t_s(f)$, $t_p(f)$=starting time and duration parameter, respectively, and $\alpha_m(f)$=intensity parameter which represents the peak value of $G_x(t, 2\pi f)$. These parameters have been determined relative to recorded accelerograms[11]. Fig. 4 shows an example of recorded and modeled evolutionary spectra.

The following regression equations are used for the model parameters to establish the prediction model for given magnitude and distance.

$$\log\hat{\alpha}_m(f)=B_0(f)+B_1(f)\cdot M-B_2(f)\cdot\log(\Delta+30) \quad \cdots\cdots (4)$$

$$\log\hat{t}_p(f)=P_0(f)+P_1(f)\cdot M+P_2(f)\cdot\log(\Delta+30) \quad \cdots\cdots (5)$$

$$\hat{t}'_s(f)=t_s(f)-t_m=S_0(f)+S_1(f)\cdot\Delta \quad \cdots\cdots (6)$$

In Eq. (6), $t'_s(f)=t_s(f)-t_m$, where t_m is the average value of $t_s(f)$ over the frequency range considered herein. Consideration of t_m is necessary since the recorded accelerograms used for the statistical analysis have been obtained only on relative reference times.

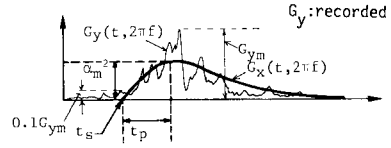

Fig. 4 Recorded and Simulated Evolutionary Spectrtra.

(2) Modification and Simplification of Estimation Equations for Model Parameters[4),14)]

A number of free rock surface motions were generated for several combinations of M and Δ by using Eqs. (2)~(6). They were converted to soil surface ground motions for a number of

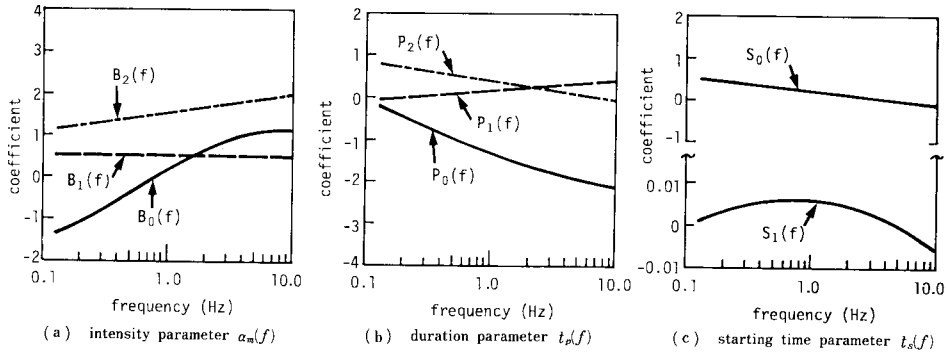

(a) intensity parameter $\alpha_m(f)$ (b) duration parameter $t_p(f)$ (c) starting time parameter $t_s(f)$

Fig. 5 Modeled Coefficients for Estimation of Model Parameters appeared in Eqs. (4)-(6).

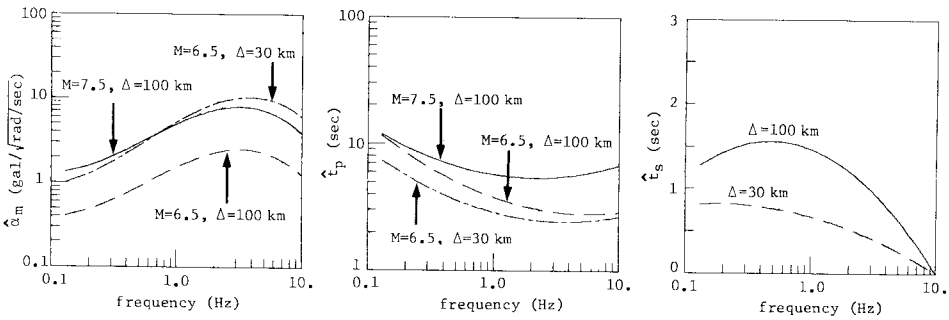

Fig. 6 Example of Model Parameters given by the EMP-IB Model.

sites dealt in this study. The peak ground motions (A_p=acceleration, V_p=velocity) of them were compared with the estimation formulas[12] which have been obtained using strong motion data recorded on soil sites. Since there were some disagreement specially around the boundary of epicentral region (Fig. 2), the coefficients $B_0(f)\sim B_2(f)$ in Eq. (4) have been modified so that the peak values A_p and V_p of ground motions converted from rock surface motions agree with that given from the estimation formulas[12].

Since the coefficients for the model parametres have some typical inclination on the frequency axis, they were modeled as a function of frequency using the least squares method[4]. The modification of the coefficients in Eq. (4) and the smoothing of the coefficients in Eqs. (4)$\sim$(6) have been discussed in detail in Ref. 4).

Table 3 Estimation Formulas for Model Parameters.

$\log\hat{\alpha}_m(f) = B_0(f) + B_1(f)\cdot M - B_2(f)\cdot\log(\Delta+30)$	
$B_0(f)=0.1553+0.175\cdot\log f-0.336(\log f)^2-0.451(\log f)^3$ $B_1(f)=0.506+0.0131\cdot\log f$ $B_2(f)=1.543+0.455\cdot\log f$	(7)
$\log\hat{t}_p(f) = P_0(f) + P_1(f)\cdot M + P_2(f)\cdot\log(\Delta+30)$	
$P_0(f)=-1.312-0.1054\cdot\log f+0.227(\log f)^2$ $P_1(f)=0.179+0.188\cdot\log f$ $P_2(f)=0.344-0.240\cdot\log f$	(8)
$\hat{t}_s(f) = t_s(f) - t_* \simeq S_0(f) + S_1(f)\cdot\Delta$	
$S_0(f)=0.439-0.978\cdot\log f$ $S_1(f)=\{0.528-0.242\cdot\log f-0.889(\log f)^2\}\times10^{-2}$	(9)

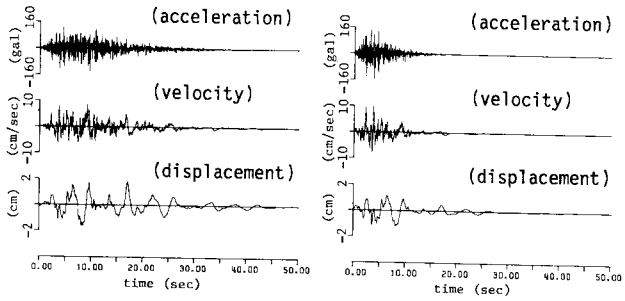

(a) M=7.5, Δ=100 km (b) M=6.5, Δ=30 km

Fig. 7 Simulated Free Roce Surface Motions by the EMP-IB Model.

The formulas for the modeled coefficients to be used in Eqs. (4)$\sim$(6) are listed in Table 3 and are shown in Fig. 5. Fig. 6 shows values of model parameters given from Eqs. (7)$\sim$(9). The simulated rock surface ground motions for two

combinations of M and Δ are shown in Fig. 7. They were generated using identical random numbers in accounting for model uncertainty.

(3) Evaluation of Prediction Uncertainty for the Model Parameters[16]

Since the EMP-IB model has been developed on the basis of the modified ground motion data, the prediction uncertainty cannot be evaluated directly from the result of the regression analysis for the model parameters. In Ref. 11) the decrease in prediction uncertainty for the intensity parameter $\alpha_m(f)$ with increase in available information on local soil conditions has been characterized. They were classified into three levels as for the available informations. The level I represents the condition for given magnitude M and distance Δ, the level II for M, Δ, and the soil parameter S_n[12], and the level III for M, Δ, S_n, and the transfer function of the ground overlying bedrocks. Assuming that the prediction uncertainty for $\alpha_m(f)$ on rock surface level is equivalent to that on soil surface level where the whole information on local soil conditions are available, the coefficient of variation δ_{α_m} for the level III may be substituted for the EMP-IB model. On the basis of the regression analysis developed in Ref. 11), the prediction uncertainty for the model parameters of the EMP-IB have been characterized and they are shown in Fig. 8. They were smoothed on the frequency axis, and the coefficient of variation δ_{α_m} for the intensity parameter $\alpha_m(f)$ and δ_{t_p} for the duration parameter $t_p(f)$ are given as $\delta_{\alpha_m}=0.426$, $\delta_{t_p}=0.650$ for the whole frequencies in the range $0.13 \leqq f \leqq 10.03$ Hz. The procedure for the simulation of ground motions incorporating model uncertainty has been discussed in detail in Ref. 3).

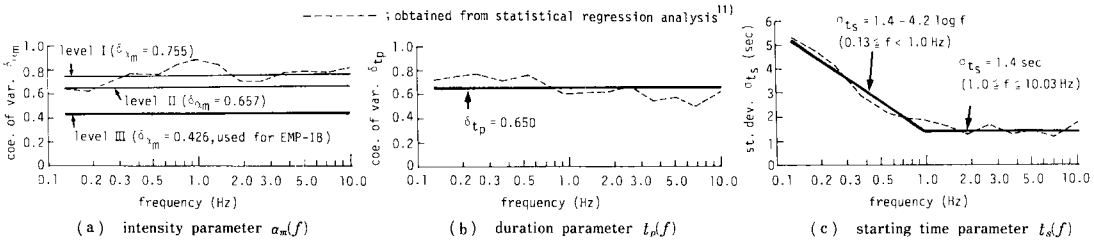

(a) intensity parameter $\alpha_m(f)$ (b) duration parameter $t_p(f)$ (c) starting time parameter $t_s(f)$

Fig. 8 Characterization of Prediction Uncertainty for Model Parameters.

4. NEAR-SOURCE GROUND MOTION PREDICTION MODEL FOR GREAT EARTHQUAKES (EMP-IIB MODEL)

(1) General Remarks

Past strong motion data from great earthquakes show that rupture direction relative to sites and geometrical condition between sites and fault make much difference in ground motion intensities and their duration. For prediction of earthquake motions for great earthquakes, therefore, physical parameters on faults and effect of successive faulting should be incorporated[21]. Herein the prediction model (EMP-IIB Model) for large-scale earthquakes is proposed, which incorporates a size of fault, rupture direction and its velocity, and seismic moment as a parameter of earthquake scale. In the EMP-IIB Model, the evolutionary spectra for great earthquakes are given from the superposition of evolutionary spectra which correspond to relatively small earthquake ($M=6.0$) in the EMP-IB Model.

Fig. 9 gives general concept[23),28)] of the model. The fault is divided into a number of small events which correspond to the unit event ($M=6.0$) in the EMP-IB Model. The arriving time lag $t_{a_{ij}}$ resulted from rupture on the fault and difference of propagation distance of ground motions, can be given in the following form.

$$t_{a_{ij}}=d_{ij}/v_r+(\Delta_{ij}-\Delta_s)/v_{pr} \quad \cdots\cdots (10)$$

In the case of deep fault, a hypocentral distance r_s in place of Δ_s and direct distance between site and each unit event r_{ij} instead of Δ_{ij} may be used.

(2) Number of Superposition N_G scaled for Seismic Moment

The number of superposition N_G of evolutionary spectra is defined. The parameter N_G represents the number of small unit events on a specific great fault. The following procedure has been performed to obtain the superposition parameter N_G.

The magnification factor $c(f)$ defined by Eq. (11) may be used for amplification value of evolutionary power spectrum.

$$c(f)=\int_0^{t_0}\sqrt{G_x(t,2\pi f)}\,dt\Big/\int_0^{t_0}\sqrt{G_x^*(t,2\pi f)}\,dt \quad \cdots\cdots (11)$$

where G_x=simulated evolutionary spectrum for the data, G_x^*=evolutionary spectrum given from the EMP-IB Model which corresponds to the earthquake magnitude $M=6.0$ and the 'same distance' of the specific data, and t_0=duration of the data. The number of superposition N_G, the average of the magnification factor $c(f)$ along the logarithmic frequency axis, is defined as

$$N_G=\int_{\log f_1}^{\log f_2} c(f)d(\log f)/(\log f_2-\log f_1) \quad \cdots\cdots (12)$$

where the lower and upper frequencies f_1, f_2 are fixed as $f_1=0.13$ Hz, $f_2=10.03$ Hz. The parameter N_G represents the number of superposition of evolutionary spectra for a standard earthquake of $M=6.0$ in the EMP-IB Model. The value N_G has been obtained for 53 components from 12 earthquakes listed in Table 4, the seismic moment M_0 of which have been given. Fig. 10 shows the relation between the number of superposition N_G and the seismic moment M_0. The parameter N_G has been scaled for M_0, and the following relation has been obtained.

$$\overline{N}_G=2.317\times10^{-12}\times M_0^{0.468} \quad \cdots\cdots (13)$$

In Eq. (13) the value M_0 which gives $N_G=1$ is given as $M_0=7.24\times10^{24}$. This value nearly coinside with $M_0=7.76\times10^{24}$ which gives $M_S=6.0$ in the relation between M_0 and the surface magnitude M_S proposed by Geller[2]. Since the JMA magnitude coinside with M_S in case of relatively small magnitude as around $M=6.0$[32], the above result supports the validity of the model.

Table 4 Fault Parameters for Major Japanese Earthquakes[26),31)].

event	date	magnitude M	seismic moment M_0 (dyn·cm)
1968 Huganada	April 4, 1968	7.0	1.8×10^{27}*
1968 Tokachi-oki	May 16, 1968	7.9	2.8×10^{28}
Tokachi, Off Shore	May 16, 1968	7.4	1.3×10^{27}*
Saitama, Center	July 1, 1968	6.1	1.9×10^{25}
Ehime, West Coast	August 6, 1968	6.6	2.0×10^{26}
Ibaragi, Off Shore	July 23, 1972	7.0	3.2×10^{26}*
1978 Izuoshima Kinkai	Jan. 14, 1978	7.0	1.0×10^{26}
Miyagi, Off Shore	Feb. 20, 1978	6.7	8.0×10^{25}
1978 Miyagiken-oki	June 14, 1978	7.4	3.1×10^{27}
1982 Urakawa-oki	March 21, 1982	7.1	2.0×10^{26}
1983 Nihonkai-Chubu	May 26, 1983	7.7	5.0×10^{27}
Nihonkai, Center	June 21, 1983	7.1	4.5×10^{26}*

* estimeted from the magnitude as $\log M_0=1.5M+16.0$ (Ref.22)

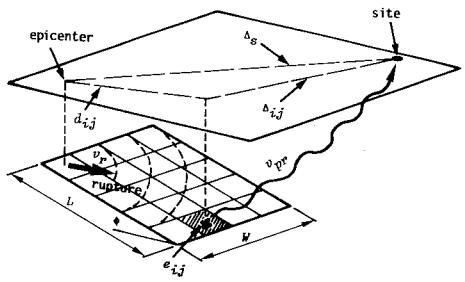

Fig. 9 Fault Modeling with Multiple Fault Ruptures.

The superposed evolutionary spectra for great earthquake is given as

$$\sqrt{G_{x_0}(t,2\pi f)}=\frac{N_G}{n_G}\beta(f,M_0)\sum_{ij}^{n_G}\sqrt{G_{z_{ij}}(t,2\pi f)} \quad \cdots\cdots (14)$$

where $G_{z_{ij}}$=evolutionary spectrum for each unit event e_{ij}, which corresponds to the earthquake of $M=6.0$, $\Delta=\Delta_{ij}$ in the EMP-IB Model. The value

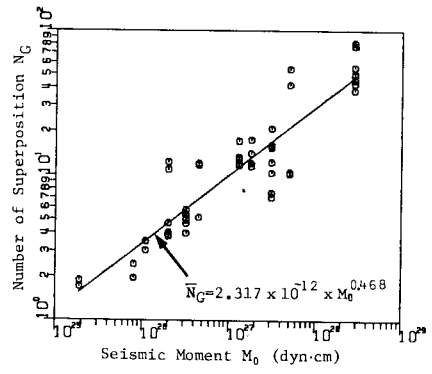

Fig. 10 Relation between Number of Superposition N_G ane Seismic Moment M_0.

N_G is generally not an integral number, therefore the number n_G which is a similar number for N_G and by which the specific fault can be divided, should be used. Then, the coefficient N_G/n_G is necessary for modification of total power. Further the correction factor $\beta(f,\ M_0)$ is necessary for superposing of each frequency component, which has been obtained from the regression of the parameter $c(f)$ on seismic moment.

The correction factor $\beta(f,\ M_0)$ has been also modeled on the frequency axis, and is given[4]

$$\beta(f,\ M_0)=10^{a_0(f)}M_0^{a_1(f)} \quad (15)$$

where

$$\left.\begin{aligned} a_0(f)&=0.948-4.60\cdot\log f \\ a_1(f)&=-0.0388+0.178\cdot\log f \end{aligned}\right\} \quad (16)$$

Fig. 11 gives a schematic description for the superposed evolutionary spectra.

The prediction uncertainty for the superposed evolutionary spectra in the EMP-IIB model can be characterized by the coefficient of variation δ_N about the regression line shown in Fig. 10. The value of δ_N has been obtained as $\delta_N=0.41$.

(3) Procedure of Earthquake Motion Prediction in the EMP-IIB Model and Its Examples

The procedure of earthquake motion prediction in the EMP-IIB Model is as follows.

1) Calculate the number of superposition N_G for given seismic moment M_0 by Eq. (13), and find the integral number n_G, by which the given fault can be devided properly according to the fault dimensions.
2) Calculate the distance Δ_{ij} and the mean arrival time $t_{a_{ij}}$ (Eq. (10)) for each unit event by using the given fault dimentions, rupture velocity v_r, and propagation velocity of seismic waves v_{pr}.
3) Calculate the evolutionary spectra $G_{z_{ij}}$ for each distance Δ_{ij} and $M=6.0$ in the EMP-IB Model (Eqs. (3), (4)~(6)). Then, superpose the evolutionary spectra $G_{z_{ij}}$ considering the arrival time lag $t_{a_{ij}}$ (Eq. (14)).
4) The ground motion time series is obtained by substituting $G_{x_0}(t,\ 2\pi f)$ for $G_x(t,\ 2\pi f)$ in Eq. (2).

Typical engineering characteristics of strong ground motions derived from the EMP-IIB Model were obtained. A number of sample earthquake motions were generated by the EMP-IIB Model for the

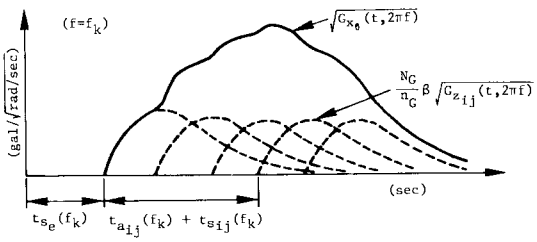

Fig. 11 Superposed Evolutionary Spectra.

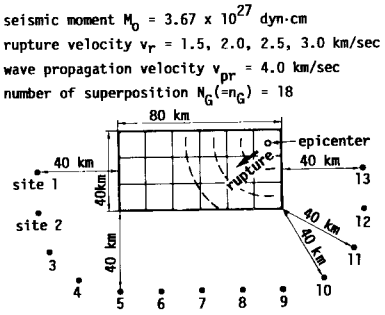

Fig. 12 Hypothetical Fault Model and Site Locations.

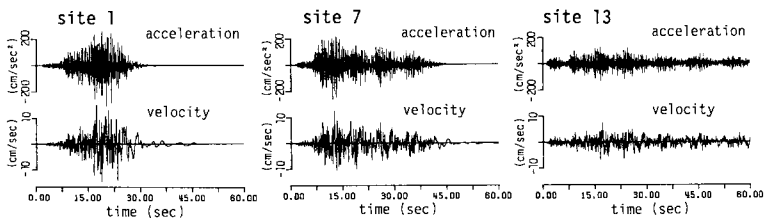

Fig. 13 Simulated Free Rock Surface Motions for Site 1, 7, and 13 in Fig. 12

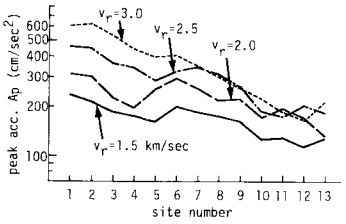

Fig. 14(a) Fluctuation of Peak Acceleration.

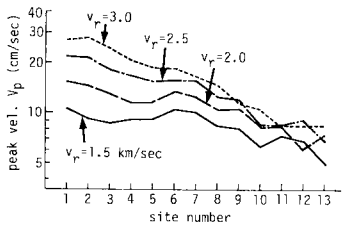

Fig. 14(b) Fluctuation of Peak Velocity.

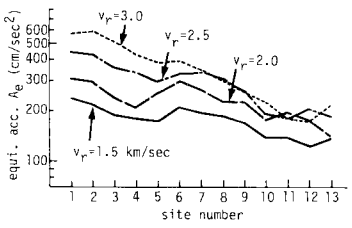

Fig. 14(c) Fluctuation of Equivalent Acceleration.

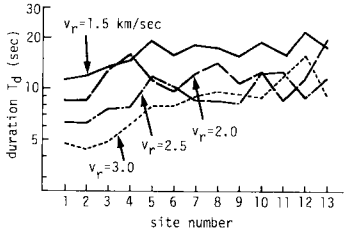

Fig. 14(d) Flrctuatıon of Ground Motion Durtion.

hypothetical fault shown in Fig. 12. Fig. 13 shows sample earthquake motions for site 1, 7, and 13. Fig. 14 (a)～(d) show the fluctuations of peak ground motions, effective peak acceleration A_e[15], and ground motion duration T_d[33] for several values of rupture velocity v_r.

5. CONCLUSIONS

Majour conclusions derived from this study may be summarized as follows.

(1) The rock surface strong motion dataset has been arranged, which consists of 91 components of major Japanese accelerograms. They are classified into 3 types of data : (i) rock surface-ground motions estimated from the accelerograms recorded on alluvial and diluvial sites, (ii) rock surface-ground motions modified from bed rock ground motions, and (iii) ground motions recorded on rock surface. In 16 components of the data in (i), the surface wave motions have been eliminated by using the simplified separation technique proposed by the authors.

(2) The nonstationary earthquake motion prediction model on free rock surface (EMP-IB Model) for given magnitude and distance has been developed by using the strong motion dataset arranged in this study. The model is also applicable for earthquake motion prediction on soil sites by considering the amplification effects of the soil overlying bedrocks.

(3) The EMP-IB Model has been extended to the prediction model for great earthquakes (EMP-IIB Model) which incorporates the effect of fault size, successive fault rupture, and rupture direction, on characteristics of ground motions. The EMP-IIB Model is based on the superposition technique of evolutionary spectra of small events that corresponds to the earthquake of $M=6.0$ in the EMP-IB Model. For the scaling of the number of superposition N_G, the seismic moment has been incorporated.

In case of earthquake motion prediction for soil deposite sites by the EMP-IB and IIB Model, it should be considered to incorperate surface wave motions into the estimated motions. Surface waves in the frequency range dealt with in this paper are mainly caused from local soil conditions near sites. Further works on this subject should be developed.

6. ACKNOWLEDGMENTS

The authors would like to express their deep appreciation to Mr. H. Saito of Japan Road Association (formarly Graduate Student at Kyoto University) for the development of rock surface-ground motion dataset and computer programs used in this study. Special appreciations are extended to the staffs of the

Port and Harbor Research Institute, Mininstry of Transport, for the strong motion data including the data from the 1983 Nihonkai-chubu Earthquake[20]. The strong motion data given from the Public Works Research Institute, Ministry of Construction are also acknowledged. The work was partly supported by Grant-in-Aid from the Japanese Ministry of Education, Science and Culture (No. 59025027, 59750352). The numerical computation has been performed on the FACOM M 382/VP 100 computer system of the Data Processing Center, Kyoto University.

REFERENCES

1) Design Seismic Load Research Group (SLG) : Corrected and Integrated Earthquake Motion Accelerograms (Graphical Information), Research Report No. 84-ST-03, School of Civil Engineering, Kyoto Univ., July 1984.
2) Geller, R. J. : Scaling Relations for Earthquake Source Parameters and Magnitudes, BSSA, Vol. 66, pp. 1501~1523, 1976.
3) Goto, H., Kameda, H. and Sugito, M. : Prediction of Strong Earthquake Motions by Evolutionary Process Model, Proc. of JSCE, No. 286, pp. 37~51, 1979.
4) Goto, H., Sugito, M., Kameda, H., Saito, H. and Ohtaki, T. : Prediction of Nonstationary Earthquake Motions for Moderate and Great Earthquakes on Rock Surface, Annuals, Disaster Prevention Research Institute, Kyoto, University, Vol. 27 B-2, 1984.
5) Hardin, B. O. and Drnevich, V. P. : Shear Modulus and Damping in Soils, Proc. ASCE, Mol. 98, SM 6, 7, 1972.
6) Haskell, N. A. : Elastic Displacements in the Near-field of a Propagating Fault, BSSA, Vol. 59, pp. 865~908, 1969.
7) Hisada, T., Ohsaki, Y., Watabe, M. and Ohta, T. : Design Spectra for Stiff Structures on Rock, 2nd International Earthquake Microzonation Conference, Vol. Ⅲ, pp. 1178~1198, 1978.
8) Izutani, Y. : A Statistical Model for Prediction of Quasi-realistic Strong Ground Motion, J. Phys. Earth, 29, pp. 537~557, 1981.
9) Japan Road Association : Design Code for Bridges, – Earthquake Registant Design , Vol. V, 1980 (in Japanese).
10) Kameda, H. and Ieiri, R. : Attenuation and Microzonation of Acceleration Response Spectra, Proc. of the 37th Annual Conference of the JSCE, No. 1, pp. 667~668, 1982 (in Japanese).
11) Kameda, H., Sugito, M. and Asamura, T. : Simulated Earthquake Motions Scaled for Magnitude, Distance, and Local Soil Conditions, Proc., 7 WCEE, Vol. 2, pp. 295~302, 1980.
12) Kameda, H., Sugito, M. and Goto, H. : Microzonation and Simulation of Spatially Correlated Earthquake Motions, Proc. of the 3rd International Earthquake Microzonation Conference, Vol. Ⅲ, pp. 1463~1474, 1982.
13) Kameda, H. : Evolutionary Spectra of seismogram by Multifiltere, Jour. Eng. Mech. Div., ASCE, Vol. 101, No. EM 6, pp. 787~801, 1975.
14) Kameda, H. and Sugito, M. : Prediction of Strong Earthquake Motions on Rock Surface Using Evolutionary Process Model, Conference on Structural Analysis and Design of Nuclear Power Plants, Port Alegre-RS, Oct. 1984. and Research Report No. 84-ST-02, School of Civil Engineering, Kyoto Univ., Sept. 1984.
15) Kameda, H. and Kohno, K. : Effect of Ground Motion Duration on Civil Engineering Structures, —Development of Equivalent Ground Acceleration EQA—," Memoirs of Faculty of Engineering, Kyoto Univ., Vol. XLV, Part 2, 1983.
16) Kameda, H. and Sugito, M. : Earthquake Motion Uncertainty as Compared between Soil Surface and Rock Surface Motions ··· Characterization using Evolutionary Process Model···, 8th International Conference on Structural Mechanics in Reactor Technology, Brussels, August, 1985.
17) Kanai, K. : Empirical equations for earthquake motion intensity, 5th Japan Earthquake Engineering Symposium, pp. 1~4 (1966) (in Japanese).
18) Katayama, T., Iwasaki, T. and Saeki, T. : Statistical Analysis of Earthquake Acceleration Response Spectra, Proc., JSCE, No. 275, pp. 29~40, 1978 (in Japanese).
19) Kawashima, K., Aizawa, M. and Takahashi, K. : Estimation of Peak Ground Motions and Response Spectra, Reports of Public Work Research Institute, No. 1993, 1983 (in Japanese).
20) Kurata, E., Fukuhara, T., and Noda, S. : Strong Motion Earthquake Records on the 1983 Nipponkai-chubu Earthquke in Port Areas, Technical Note of the Port and Harbor Research Institute, Ministry of Transport, No. 458, 1983.
21) Midorikawa, S. and Kobayashi, H. : On Estimation of Strong Motion with Regard to Fault Rupture, 2nd International Earthquake Microzonation Conference, Vol. Ⅱ, pp. 825~836, 1978.
22) Muramatsu, I. and Irikura, K. : Synthesis of Strong Earthquake Motions over a Wide Frequency Range, J. of Natural Disaster Science, Vol. 4, No. 2, 1982.
23) Ohsawa, I, Kameda, H. and Sugito, M. : Preediction Model for Near-Source Ground Motions for Great Earthquakes by Fault Division Model, Proc. of the 35th Annual Conference of the JSCE, No. 1, pp. 376~377, 1980 (in Japanese).
24) Saito, H. : Nonstationary Earthquake Motion Prediction on Rock Surface, Master's Thesis of Kyoto University, No. 1407, 1984

(in Japanese).

25) Schnabel, R. B., Lysmer, J. and Seed, H. B. : SHAKE A Computer Program for Earthquake Response Analysis of Holizontally Layered Sites, EERC, 72~12, 1972.

26) Seno, T., Shimazaki, K., Somerville, P. and Eguchi, T. : Rupture Process of the Miyagiken-oki Earthquake of June 12, 1978, Submitted to Phys. Earth. Planet. Inter., 1979.

27) Sugito, M., Goto, H. and Aikawa, F. : Simplified Separation Technique of Body and Surface Waves in Strong Motion Accelerograms, Proc. of JSCE, No. 350/ I -2, pp. 380~386, 1984.

28) Sugito, M. and Kameda, H. : Prediction of Near-Source Ground Motions for Great Earthquakes from Superposed Evolutionary Process Models, Proc. 8 WCEE, Vol. II, pp. 509~516, 1984.

29) Toki, K. and Sato, T. : Simulation of Strong Motion Seismograms by Autoregressive Moving Average Process, Disaster Prevention Research Institute, Annuals, No. 23 B-2, pp. 1~12, 1980 (in Japanese).

30) Tsuchida, H., Kurata, E., Yamada, T., Ishizaka, T. and Yokoyama, Y. : Soil Profiles at Strong Motion Stations, Technical Note of the Port and Harbor Research Institute, Ministry of Transport, No. 34, 107, 156, 298, 351, 1967-1980 (in Japanese).

31) Usami, T. : Catalogue of Japanese Disastrous Earthquakes, University of Tokyo Press, 1975 (in Japanese).

32) Utsu, T. : Relationship between Earthquake Magnitude Scales, Bull. Earthq. Res. Inst., Vol. 57, pp. 465~497, 1982 (in Japanaese).

33) Vanmarke, E. H. and Lai, S-S. P. : Strong Motion Duration and RMS Amplitude of Earthquake Records, BSSA, Vol. 70, No. 4, pp. 1293 ~1307, 1980 (in Japanaese).

(Received November 26 1984)